Arctic, Antarctic, and Alpine Research, Vol. 40, No. 4, 2008, pp. 624–637

Paleoecological Evidence for Transitions between Contrasting Landforms in a Polygon-Patterned High Arctic Wetland

Christopher J. Ellis‡*
*Line Rochefort**
Gilles Gauthier† and*
Reinhard Pienitz†

*Département de phytologie et Centre d'études nordiques, Pavillon Paul-Comtois, Université Laval, Québec, Qc., G1K 7P4, Canada
†Département de géographie et Centre d'études nordiques, Pavillon Abitibi-Price, Université Laval, Québec, Qc., G1K 7P4, Canada
‡Corresponding author. Present address: Royal Botanic Garden Edinburgh, 20A Inverleith Row, Edinburgh, EH3 5LR, U.K.
c.ellis@rbge.org.uk

Abstract

The formation of many arctic wetlands is associated with the occurrence of polygon-patterned permafrost. Existing scenarios to describe and explain surface landforms in arctic wetlands (low-center and high-center polygons and polygon ponds) invoke competing hypotheses: a cyclic succession (the thaw-lake hypothesis) or a linear succession (terrestrialization). Both hypotheses infer the predictable development of polygon-patterned wetlands over millennia. However, very few studies have applied paleoecological techniques to reconstruct long-term succession in tundra wetlands and thereby test the validity of existing hypotheses. This paper uses the paleoecological record of diatoms to investigate long-term development of individual polygons in a High Arctic wetland. Two landform processes were examined: (1) the millennial-scale development of a polygon-pond, and (2) the transition from low-center to erosive high-center polygons. Diatom assemblages were quantified from habitats associated with contrasting landforms in the present-day landscape, and used as an analog to reconstruct past transitions between polygon types. On the basis of this evidence, the paleoecological record does not support either of the existing models describing the predictable succession of polygon landforms in an arctic wetland. Our results indicate a need for greater paleoecological understanding, in combination with *in situ* observations in present-day geomorphology, in order to identify patterns of polygon wetland development and elucidate the long-term drivers of these landform transitions.

DOI: 10.1657/1523-0430(07-059)[ELLIS]2.0.CO;2

Introduction

The occurrence of permafrost at high latitudes enables the widespread development of arctic and subarctic wetlands (Tarnocai and Zoltai, 1988; Bliss, 1997); i.e. in low-lying areas, drainage of snowmelt is impeded by perennially frozen ground. In the High Arctic such wetlands are frequently referred to as oases, being comparatively rich in plant diversity with high productivity (Bliss and Matveyeva, 1992), and they provide important summer habitat for muskox and large populations of migratory birds (Bliss and Matveyeva, 1992; Bliss, 1997). The cold and wet soil conditions in arctic wetlands preclude decomposition, and as organic matter accumulates each year, the frost table rises upwards, incorporating peat into the aggrading permafrost (Billings, 1987; Gorham, 1991; Michaelson et al., 1996; Vardy et al., 2000). Peat-rich soils associated with arctic wetlands have contributed a net sink for carbon during the Holocene and are estimated to store >97% of the tundra carbon reserve comprising ca $180-190 \times 10^{15}$ g of soil-C, (Post et al., 1982; Oechel and Vourlitis, 1994). Given the incidence of suitably wet soil moisture conditions, the formation of ice wedges has resulted in the development of patterned ground over vast areas of the arctic landscape (Leffingwell, 1915; Lachenbruch, 1966; Péwé, 1966; Mackay, 1990, 2000). The accretion of peat and eolian sediments is therefore accompanied by the upward growth of syngenetic ice wedges (Harry and Gozdzik, 1988; Mackay, 1990, 1999) to form polygon-patterned wetland (Tarnocai and Zoltai, 1988; Bliss, 1997).

The landforms associated with polygon-patterned wetlands can be broadly divided into three types (Péwé, 1966; Billings and Peterson, 1980): low-center polygons (raised polygonal ridges surrounding a lower, wetter center), polygon ponds (raised polygonal ridges surrounding a pool), and high-center polygons (a raised, domed center surrounded by a polygonal network of troughs) (Fig. 1). Scenarios describing the long-term development of these periglacial landforms are based primarily on observations made in the present-day landscape of what are inferred to be chronosequence stages. Accepted explanations for the long-term development of arctic wetlands invoke directional change (cf. Svoboda and Henry, 1987; Bliss, 1997), though they are contrasting in pattern. For example, the widely accepted "thaw-lake cycle hypothesis" (Fig. 2) invokes a cyclic succession of vegetation over ca. 3000 yr (Britton, 1957; Billings and Peterson, 1980), though it contrasts with an inferred linear sequence of terrestrialization (Zoltai and Tarnocai, 1975) in which peat accumulation in polygon centers is thought to cause the gradual and linear transition from wet low-center polygons to dry high-center polygons. Elements of the thaw-lake cycle are supported by studies in paleoecology and periglacial geomorphology: e.g. the gradual inundation of low-center polygons as ridges become higher (Seppälä et al., 1991) and the regeneration of ice wedges on drained lake beds (Mackay, 1986, 1999). In contrast, a linear sequence of terrestrialization involving the development of high-center from low-center polygons has been supported by paleoecological reconstruction (Ovenden, 1982; Vardy et al., 1997). Determining the relative importance of these contrasting successional patterns (e.g. linear versus cyclic) is an essential prerequisite to correctly understand the long-term function of arctic terrestrial wetlands. The shift between

1523-0430/08 $7.00

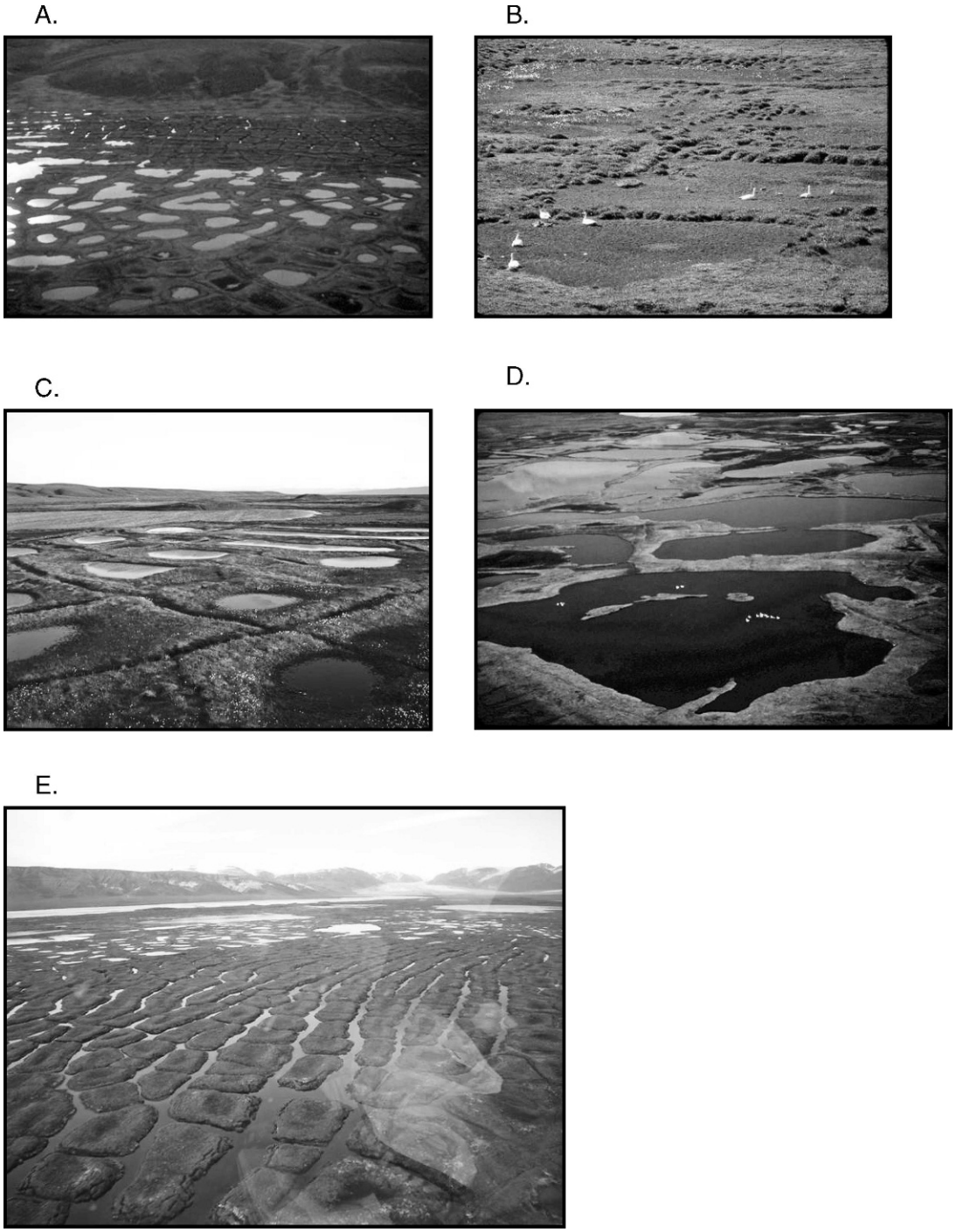

FIGURE 1. (A) Contrasting zones characterized by low-center polygons (lower right foreground), polygon ponds (center) grading into thaw lakes (center-left), and high-center polygons (background) at the study site in Qarlikturvik Valley, Bylot Island; (B) low-center polygons; (C) polygon ponds; (D) thaw lakes; and (E) high-center polygons.

landforms is associated with major hydrologic and vegetation differences (cf. Fig. 1) and can have significant impact on ecosystem function (i.e. the C-flux; cf. Billings et al., 1982, 1983; Johnson et al., 1996).

This paper attempts to confirm or refute the validity of linear versus cyclical models describing long-term succession in a High Arctic wetland, using diatoms as a tool for paleoenvironmental reconstruction (cf. Battarbee et al., 2001). A quantitative description of diatoms from landforms in the present-day wetland is used as an analog to reconstruct past hydrologic change, i.e. the development of a polygon-pond and a series of local shifts to drier high-center polygon conditions. We thus examine the sequence of hydrologic change for key stages during landform transitions, and ask:

(1) Does the paleoecological development of a polygon pond match with a predictable hydrologic sequence consistent with the transition from low-center polygon, to pond, to thaw lake? (i.e. stages C → D → E; Fig. 2)

(2) Is the transition to a high-center polygon consistent with slow, linear terrestrialization? Alternatively, is the transition to a high-center polygon consistent with a preceding period of lake formation? (i.e. stages E → F; Fig. 2)

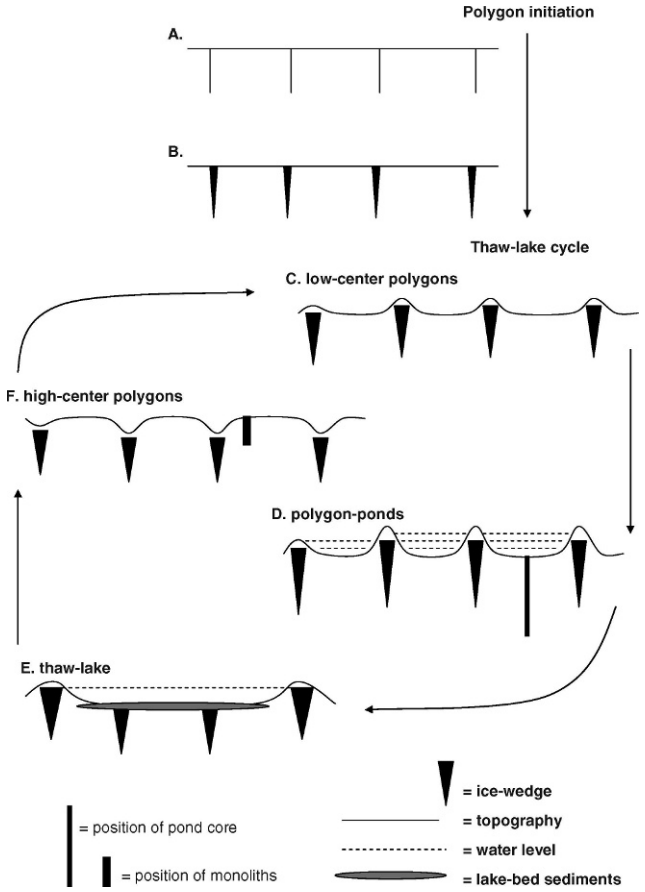

FIGURE 2. A representation of the "thaw-lake cycle hypothesis," with stages of geomorphologic development represented in cross section. The initiation of ice wedges occurs where ground newly exposed to severe winter temperatures undergoes thermal contraction, cracking into a series of polygonal fissures (A). Meltwater entering the fissures during spring and summer thaw will subsequently refreeze, forming veins of ice (B). Recurrent cracking of the same ice veins, their inundation by meltwater and subsequent refreezing and fracture cause incremental addition and growth to form wedge-shaped bodies of ground ice. The progressive expansion of ice wedges displaces surrounding cryosols, causing with the thermal expansion of adjacent ground the development of dry ridges, which thus surround lower, wetter polygon-centers—low-center polygons (C). In depositional environments "syngenetic" ice wedges grow vertically as the permafrost table rises with the accretion of sediments. Growth of syngenetic wedges is enabled by the long-term aggradation of peat-rich sediment, occurring under limiting conditions of slow, continuous sedimentation and repeated frost cracking. In lower, wetter areas the persistence of water in low-center polygons increases, with the eventual formation of polygon ponds (D). The gradual wind and water erosion of ridges causes small ponds to coalesce (E), resulting in deeper and larger polygon ponds and eventually thaw lakes. During the period of inundation the upper parts of ice wedges will thaw, though lake-bed sediments will insulate submerged ice wedges where the lower part remains embedded in the permafrost. Larger ponds and thaw lakes are increasingly susceptible to capture and drainage by the headward extension of adventitious streams. With inevitable drainage the barren sediments appear as erosive high-center polygons: troughs replace ridges where melting of the upper ice wedges has resulted in subsidence (F). Thermokarst erosion may initially cause further break-up of high-center polygons, deepening the troughs until vegetation recovery and sedimentation ultimately enable the rejuvenation of intact ice wedges, with the reestablishment of low-center polygons and the beginning of a new cycle (C). Our sampling strategy aimed to reconstruct landform transitions during this cyclical development, with a permafrost core collected from the center of a polygon pond and monoliths from high-center polygons.

Study Site

The study site was located on terraces lying to the south of Qarlikturvik Valley in western Bylot Island (Fig. 3), within the Simirlik National Park (73°08′N; 80°00′W), part of the Canadian Arctic Archipelago between latitudes 72° and 74°N and longitudes 75° and 82°W. The general character of Qarlikturvik Valley and details of the study site are provided by Allard (1996) and Fortier and Allard (2004).

The valley terraces comprising the study site have developed during the post-glacial accretion of eolian sands and silts and the concurrent deposition of peat, initiated at ca. 3500–4000 yr BP; for process descriptions see Allard (1996) and Fortier and Allard (2004). Syngenetic growth of ice wedges in the aggrading sediments has resulted in the extensive development of polygon-patterned ground, and the terraces include a range of associated landforms (Fig. 1): low-center and high-center polygons, polygon-ponds, and thaw lakes (cf. Billings and Peterson, 1980). The polygon complex is fed by meltwater from the hills to the south, and the vegetation is dominated by sedges (e.g. *Carex aquatilis* var. *stans*, *Eriophorum scheuchzeri*), grasses (e.g. *Arctagrostis latifolia*, *Dupontia fischeri*, *Pleuropogon sabinei*), and fen mosses (e.g. *Drepanocladus* spp., *Aulocomnium* spp.).

Methods

PERMAFROST CORES

A single sediment profile 147 cm long in depth was extracted from the center of a frozen polygon pond in June 1999 (BY-Pond) (Fig. 3c). First, sediments from the active layer (to ca. 30 cm depth) were sampled as 2 cm slices cut with a knife from an unfrozen peat monolith (ca. 2 cm deep × 10 cm × 10 cm). Second, permafrost sediment was collected as contiguous 5 cm diameter, 50 cm segments, using a machine-driven corer (built by M. Allard, Université Laval). The corer was drilled vertically into the sediment until the chamber was full, recovered and the sediments removed as a single frozen column. This process was repeated until the entire depth of organic-rich sediment had been sampled down to an underlying layer of marine clay. Cored sections were examined in the field to ensure that sediments were horizontally bedded and undisturbed (cf. Fortier and Allard, 2004). The frozen 50 cm sections were cut where possible into 2 cm slices which were cleaned around their exposed outer faces (to prevent contamination), and sealed in labeled polyethylene bags. Samples were stored in a dark cooler box packed with ice for the remainder of the field season (eight weeks). On returning to the laboratory, samples were stored in the dark at 4 °C.

Three short monoliths were cut from the exposed flanks of eroded high-center polygons. Loose material was cleaned away from the eroding polygon flanks to expose a vertical face. Contiguous slices of sediment, ca. 1 cm deep × 10 cm × 10 cm, were sampled from the cleaned face, downwards from the polygon surface. Stratigraphic patterns around the back and sides of the each monolith were inspected to ensure that the sediments were approximately linear and undisturbed by cryogenic turbation (cf. Fortier and Allard, 2004). Slices were initially cut in early July 2000, from one polygon at the center of three different high-center

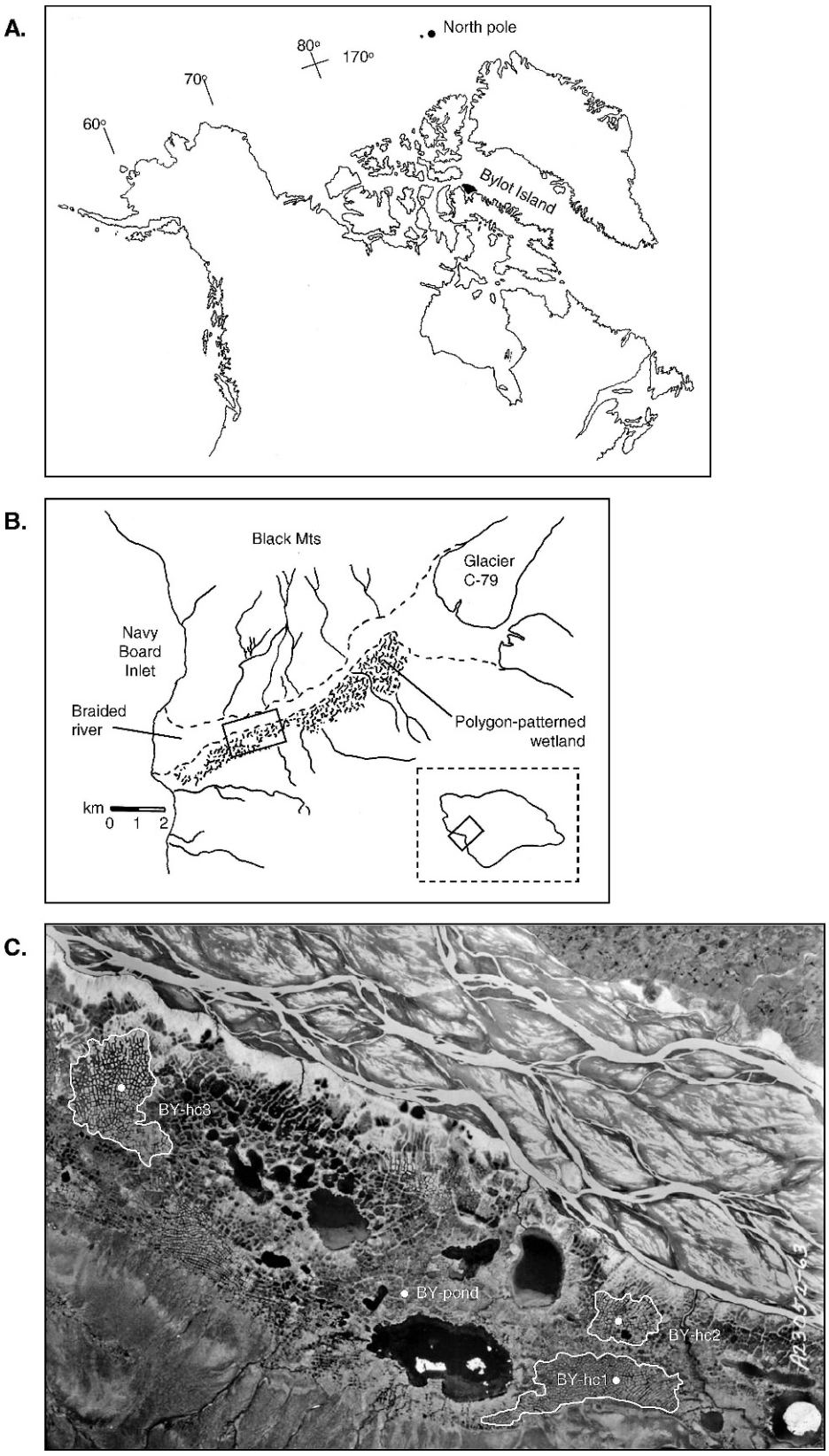

FIGURE 3. (A) The location of Bylot Island in the Canadian Arctic Archipelago; (B) the study site to the south of Qarlikturvik Valley, western Bylot Island; and (C) the permafrost core (BY-Pond) and monoliths (BY-hc1, -hc2, and -hc3) sampled from a central location within three delimited high-center polygon zones.

polygon zones (Fig. 3c). Monoliths were revisited weekly, and further slices were collected during the summer as the active layer deepened. Final monoliths were labeled BY-hc1, -hc2, and -hc3, and varied between 22 cm and 28 cm in depth.

ANALOG DIATOM ASSEMBLAGES

To quantify wetland diatom assemblages, five samples were collected in late July and early August 2000 from five contrasting landforms within the present-day polygon complex: i.e. moss mats

TABLE 1

Radiocarbon dates for permafrost core BY-pond and monoliths BY-hc1, -hc2, and -hc3, Qarlikturvik Valley, Bylot Island (73°08′N; 80°00′W). Calibrated ages were calculated using the computer program INTCAL 98 (Stuiver et al., 1998).

Core	Horizon (cm)	Code	Conventional age	Calibrated age (1 δ range)
BY-pond	61–63	Beta-143340	1990 ± 50 yr BP	1930 cal. yr BP (1995–1885)
BY-hc1	9–10	UL-2373	1710 ± 90 yr BP	1625 cal. yr BP (1730–1520)
BY-hc2	21–22	UL-2374	1690 ± 90 yr BP	1565 cal. yr BP (1710–1420)
BY-hc3	6–7	UL-2392	700 ± 100 yr BP	640 cal. yr BP (730–555)

from high-center polygons, low-center polygon flanks and centers, and the upper sediment layers from polygon ponds and thaw lakes (cf. Figs. 1 and 2). Lentic sediments were collected using a surface sediment sampler (based on a design by Benoni and Enell; Fig. 8.3 *in* Aaby and Digerfeldt, 1986). Samples were sealed in labeled polyethylene bags and stored in a dark cooler box packed with ice for the remainder of the field season (four weeks). On returning to the laboratory samples were stored in the dark at 4 °C.

LABORATORY ANALYSIS—DIATOMS

Diatom analysis was targeted to the analog samples collected from present-day wetland habitats and the horizontally bedded stratigraphic sections from core BY-Pond (0–92 cm) and monoliths BY-hc1, -hc2, and -hc3.

Siliceous microfossils (diatoms and chrysophyte cysts) were extracted from ca. 0.5 cm^3 of sediment and placed into a 250 mL beaker with an initial 30 mL of hydrogen peroxide (30% H_2O_2). The sediment was macerated and gently heated. Hydrogen peroxide was added in small amounts until all organic material had oxidized and the remaining mineral residue topped-up to 80 mL with distilled water. This mixture was stirred gently and transferred by pipette (excluding therefore the larger mineral fraction) into a second beaker, which was covered and left to settle for 48 h. Supernatant liquid was gently removed with a pipette and the deposited sediment washed into a 20 mL glass vial with distilled water. Vials were sealed and stored at 4 °C until analysis.

The mixture of sediment-distilled water was gently shaken, and a drop of liquid was evaporated onto cover-slips and mounted onto slides using Naphrax© mounting medium. Diatoms were identified and counted as transects across the slide, at ×1000 magnification using phase contrast microscopy on an Olympus BX-40. The taxonomy of arctic diatoms is poorly defined, and identification is according to Krammer and Lange-Bertalot (1986, 1988, 1991a, 1991b) and Fallu et al. (2000). A minimum of 500 diatoms was counted for the present-day samples, though it was possible to count a minimum of only 150 diatoms for samples preserved in the stratigraphic record. Values for diatom taxa and chrysophyte cysts are calculated as the percentage of the total diatom count (% TDC).

RADIOCARBON DATING

Material was radiocarbon dated from core BY-Pond and BY-hc1 to -hc3, at individual horizons delimiting a significant change in the stratigraphic record. Samples were pretreated before being submitted for radiocarbon analysis, to prevent contamination by carbon-rich Tertiary deposits (Gajewski et al., 1995), which occur on Bylot Island adjacent to and within the catchment area of the sampling site (Klassen, 1993). For BY-Pond a sediment sample of ca. 2 cm^3 was washed in distilled water and sieved through a 0.3 mm sieve. In the absence of woody remains, bryophyte stems and leaves were collected from the organic residue and rinsed in distilled water. They were dried at 60 °C and samples of ≥0.1 g submitted to Beta Analytic Ltd (Miami, Florida, U.S.A.) for radiocarbon analysis by accelerator mass spectrometry (AMS). For each of the high-center monoliths (BY-hc1, -hc2, and -hc3), a bulk sediment sample was submitted to the radiocarbon laboratory at Université Laval for dating by liquid scintillation.

Results of the radiocarbon analysis are presented in Table 1. Conventional radiocarbon ages (yr BP) were calibrated using INTCAL 98 (Stuiver et al., 1998) and are presented in the text as calibrated years before present (cal. yr BP).

STATISTICAL ANALYSIS

The proportion of diatom taxa (% TDC) was arcsine–square root transformed prior to analysis (McCune and Grace, 2002). Variation in diatom communities from landforms in the present-day polygon complex was summarized first using detrended correspondence analysis (DCA: implemented in PcOrd; McCune and Mefford, 1999) to examine compositional change, and second using the Shannon index (H′) as a measure of assemblage diversity (Magurran, 2003). Contrasts between diatom communities (DCA axis one scores, and values of H′) were compared using one-way analysis of variance, with least square difference to identify significant contrasts (implemented using Genstat v. 7.1, 2003: VSN International Ltd., Oxford, U.K.). Indicator species analysis (Dufrêne and Legendre, 1997) was used to identify diatom taxa associated with contrasting wetland landforms (implemented in PcOrd; McCune and Mefford, 1999). Statistical significance of indicator species was examined using a Monte Carlo permutation test with 10,000 iterations used to estimate significance ($p < 0.05$).

We aimed to compare the diatom composition of paleoecological strata to the composition of analog samples, though basing this comparison on the passive treatment of diatoms preserved in sub-fossil assemblages and allowing for potential losses caused by decomposition. Diatom composition of paleoecological strata was compared to that of analog communities by applying weighted averaging (WA) ordination to sub-fossil assemblages (Curtis and McIntosh, 1950, 1951), where taxon weight (W_i) is the respective score along the primary orthogonal axis derived using DCA, and A_{ij} is the abundance of diatom species i in stratigraphic horizon j:

$$S_j = \sum [A_{ij} * W_i] / \sum A_{ij} \quad (1)$$

The WA ordination of sub-fossil diatom assemblages can be used therefore to tentatively reconstruct landform and hydrologic setting, incorporating the comparison of WA scores against DCA sample scores derived for diatom communities in present-day habitats. The level of statistical significance was set at $p < 0.05$.

Results

Sixty-one diatom taxa were identified from moss mats and surface sediments collected from the present-day polygon complex (Appendix 1). Indicator species analysis identified 43 diatom taxa which were significantly associated with a given landform (Figs. 4a and 4b). Accordingly, analysis by DCA effectively summarized variation between diatom communities (Fig. 5). Orthogonal axis one ($\Delta = 0.545$) explained 27% of variation in the dataset ($R^2 = 0.27$), and there were significant differences in axis one scores between diatom assemblages sampled from contrasting landforms ($F = 37.87$, $df_1 = 4$, $df_2 = 4$, $p < 0.001$), with DCA axis one scores significantly different for four out of five landforms. There was no significant difference in axis one scores between low-center polygon centers and flanks. The diversity index (H′) identified only slight and non-significant differences in diatom community diversity between landforms representing low-center polygons, polygon ponds, and thaw lakes, with large over-lap in values of H′ (Fig. 5). However, there was a large and significant difference between the relatively more diverse communities associated with these landforms and less diverse communities sampled from high-center polygons ($F = 52.92$, $df_1 = 4$, $df_2 = 4$, $p < 0.001$).

PALEOENVIRONMENTAL RECONSTRUCTION

It was possible to consistently count a minimum of only 150 diatoms from sub-fossil samples (compared to 500 diatoms for analog samples), pointing to an effect of decomposition on paleoecological information. For this reason, the use of WA scores to passively compare preserved diatom assemblages with modern analogs is appropriate, enabling a comparison based on sub-fossil diatoms remaining intact within the permafrost sediment, and allowing for decay-related change in the paleoecological record. Significant differences in DCA scores between diatom communities sampled from contrasting landforms (Fig. 5) support our application of species scores along DCA axis one, used as weights to calculate a WA score (S_j) for sub-fossil diatom assemblages. We believe WA scores provide for each stratigraphic horizon a reasonable estimate of past environmental conditions, enabling the summary reconstruction of contrasting landforms and hydrologic setting during polygon development. Applied to horizons sampled from BY-Pond (Fig. 6), the diatom paleorecord provides evidence of changing hydrologic conditions, with at least two periods of relative dryness (sub-fossil diatom assemblages comparable to present-day communities from low-center polygon centers) intercalated between periods of wetness (i.e. with sub-fossil diatom assemblages analogous to communities sampled from fully aquatic polygon ponds). This application of WA scores is supported by shifts in the stratigraphic record of diatom indicator species (cf. Fig. 4) during development of the polygon pond (Fig. 6), with peaks in the occurrence of diatom taxa indicative of drier conditions (e.g. *Pinnularia brevicostata*, *P. sylvatica*, and *P. viridis*) contrasted against % TDC of taxa indicating fully aquatic conditions (e.g. *Cymbella ventricosa* var. *groenlandicum*, *Navicula vulpina*, and *N. pupula* syn. *Sellaphora*). The paleoecological record is disrupted between ca. 60 cm and 40 cm depth by a layer of segregation ice, though the radiocarbon date at 61–63 cm depth (ca. 1930 cal. yr BP; Table 1, Fig. 6) suggests reconstructed variation in hydrology and landform have occurred over millennia.

Transitions to high-center polygon conditions in BY-hc1, -hc2, and -hc3 can be tentatively identified as a shift in the diversity of sub-fossil diatom assemblages, from values of H′ between 2.5 and 3.5 (comparable to communities from non-eroded polygons in the present-day wetland; Fig. 5) to less than 1.75 (Fig. 7). This shift in diversity is not corrected for time differences between samples (i.e. rates of sediment growth), or contrasting rates of decomposition between polygon types, and should be treated with appropriate circumspection. However, the shift in diversity is contemporaneous with a transition in WA scores: from evidence of polygon-pond conditions (preceding the shift to a high-center polygon) to a steep trend indicating drying of the polygon-surface and supported by an increase in % TDC of the indicator species *Pinnularia borealis* (cf. Figs. 4a and 7). The sampling failed to capture the full transition in diatom composition to high-center polygon conditions because too few diatoms were preserved in the uppermost strata. Nevertheless, radiocarbon dates identify the timing of a shift between polygon ponds and high-center polygons (Table 1, Fig. 7).

Discussion

Detailed geomorphologic study of the Qarlikturvik Valley polygon complex on Bylot Island has confirmed the local presence of horizontally bedded strata in the center of polygons (Fortier and Allard, 2004). These conditions provide an environment suitable to paleoecological reconstruction and the opportunity to study the long-term development of polygon-patterned tundra. Accordingly, previous studies in this polygon complex have sought to identify the relative importance of regional climate change and local geomorphologic and vegetation processes during recurrent development of low-center polygons (Ellis and Rochefort, 2004, 2006) and have attempted paleoenvironmental reconstruction of moisture and historic wind patterns (Fortier et al., 2006). This study extends previous investigations by examining paleoecological evidence for transitions between polygon landforms, and asks whether these transitions are consistent with existing successional scenarios.

The thaw-lake cycle hypothesis (Britton, 1957; Billings and Peterson, 1980) suggests that complete cyclical transition (cf. Fig. 2: low-center polygon → polygon pond → thaw lake → high-center polygon → low-center polygon) will occur over a period of ca. 3000 yr (Billings and Peterson, 1980). The developmental period encompassed by BY-Pond (>2000 yr; Fig. 6) should be sufficient to determine a sequence of landform shifts on a time scale that is comparable to the inferred process of cyclical succession. In contrast to the thaw-lake cycle hypothesis, our evidence suggests that the polygon pond examined has not (over an equivalent time scale) undergone the inevitable coalescence and increase in permanency leading predictably towards thaw-lake conditions. The pond examined appears to have persisted over millennia as a stable unit, though incorporating periods during which it has undergone a process of increased drying and regression towards low-center polygon conditions (Fig. 6). While there is abundant physical evidence for the active coalescence of ponds into thaw lakes across the wider surface of the polygon complex (Figs. 1 and 3c), this process may occur with less predictability than inferred by a strict interpretation of the thaw-lake cycle. The thaw-lake cycle may fail to account for the potential longevity of polygon ponds at our study site, and their fluctuation between wetter and transitional drier conditions following pond formation. In addition, diatom evidence from the high-center monoliths (BY-hc1, -hc2, and -hc3) suggests that in all three instances polygon-pond conditions preceded the rapid transition to high-center polygons (Fig. 7). This contrasts with

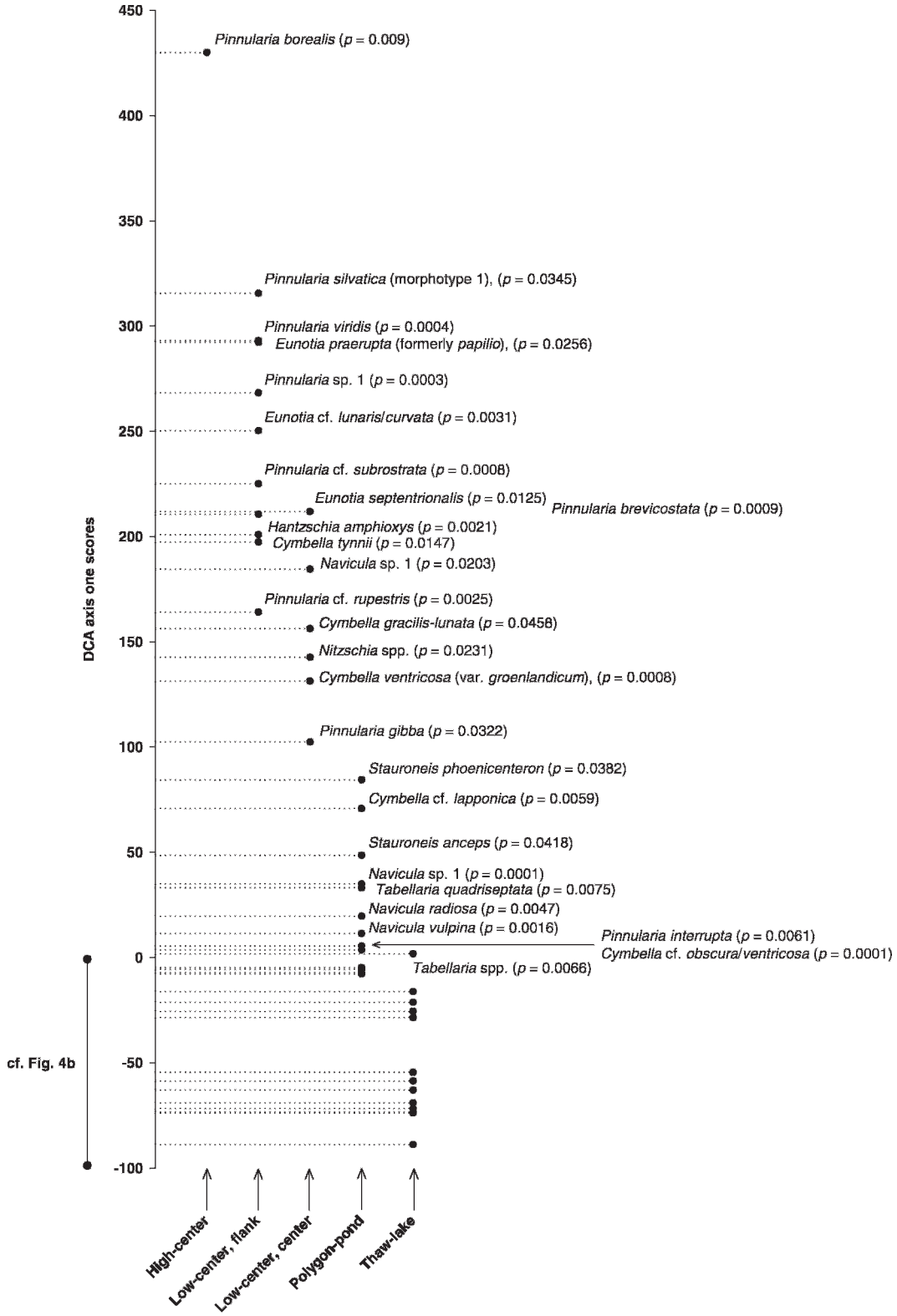

FIGURE 4. (A) Alignment of diatom indicator taxa along DCA axis one (cf. Fig. 5); showing affinities with contrasting landforms and the statistical significance of indicator values.

both the thaw-lake cycle hypothesis (Fig. 2), and the proposed sequence of gradual terrestrialization (Zoltai and Tarnocai, 1975). Instead, the paleoecological reconstruction presented here indicates that high-center polygons may be formed by the degradation of ice wedges surrounding polygon ponds, and the subsequent collapse of ridges to form troughs. Following this transition, high-center polygons may persist for many centuries (or even millennia) without the subsequent rejuvenation of actively aggrading low-center polygons (Fig. 7).

We believe this study presents the first paleoenvironmental evidence to directly address specific landform transitions in a High Arctic polygon-patterned wetland. The results of the study weaken the widespread applicability of generalized scenarios describing the predictable succession of landforms in polygon-patterned

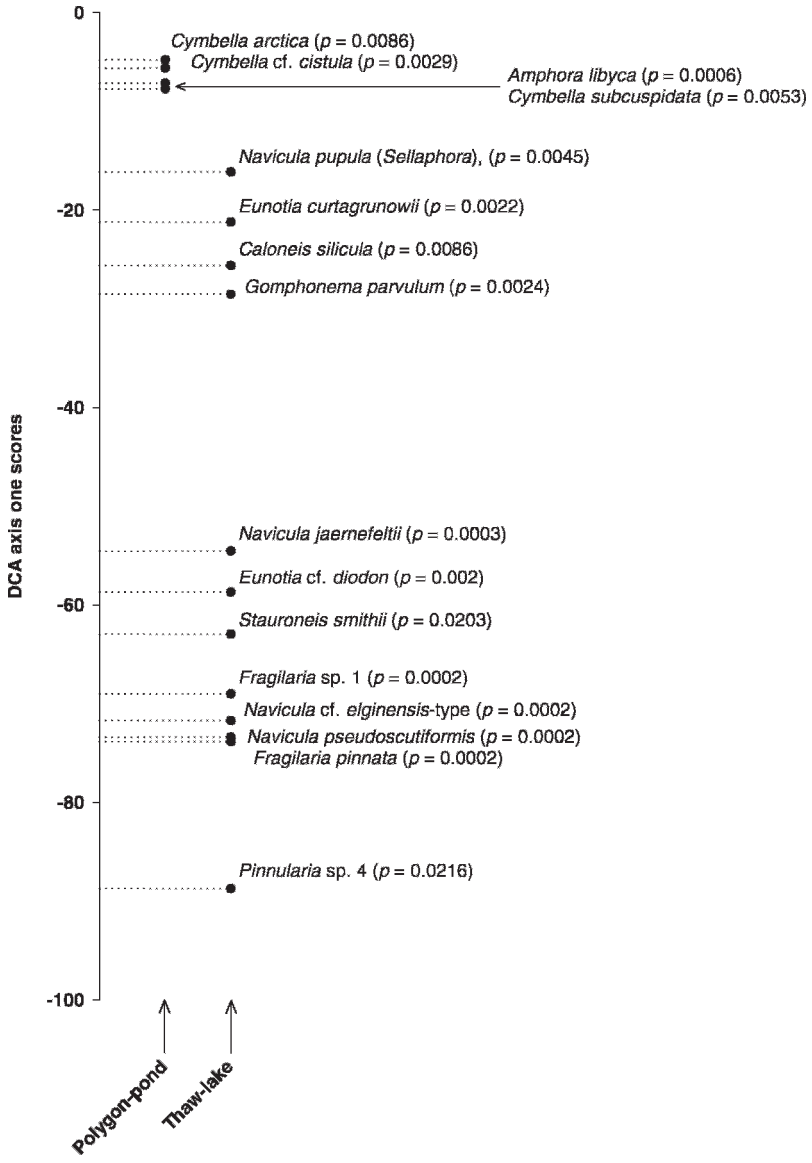

FIGURE 4 (continued). (B) Alignment of diatom indicator taxa along DCA axis one (cf. Fig. 5); showing affinities with contrasting landforms and the statistical significance of indicator values.

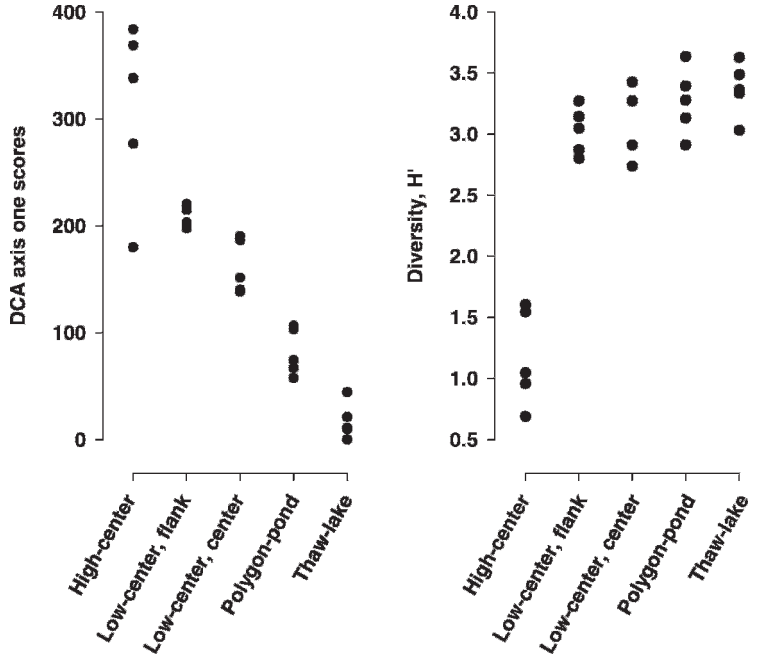

FIGURE 5. DCA axis one scores and values of diversity H′ compared between diatom communities sampled as analogues from contrasting landforms in the present-day polygon complex.

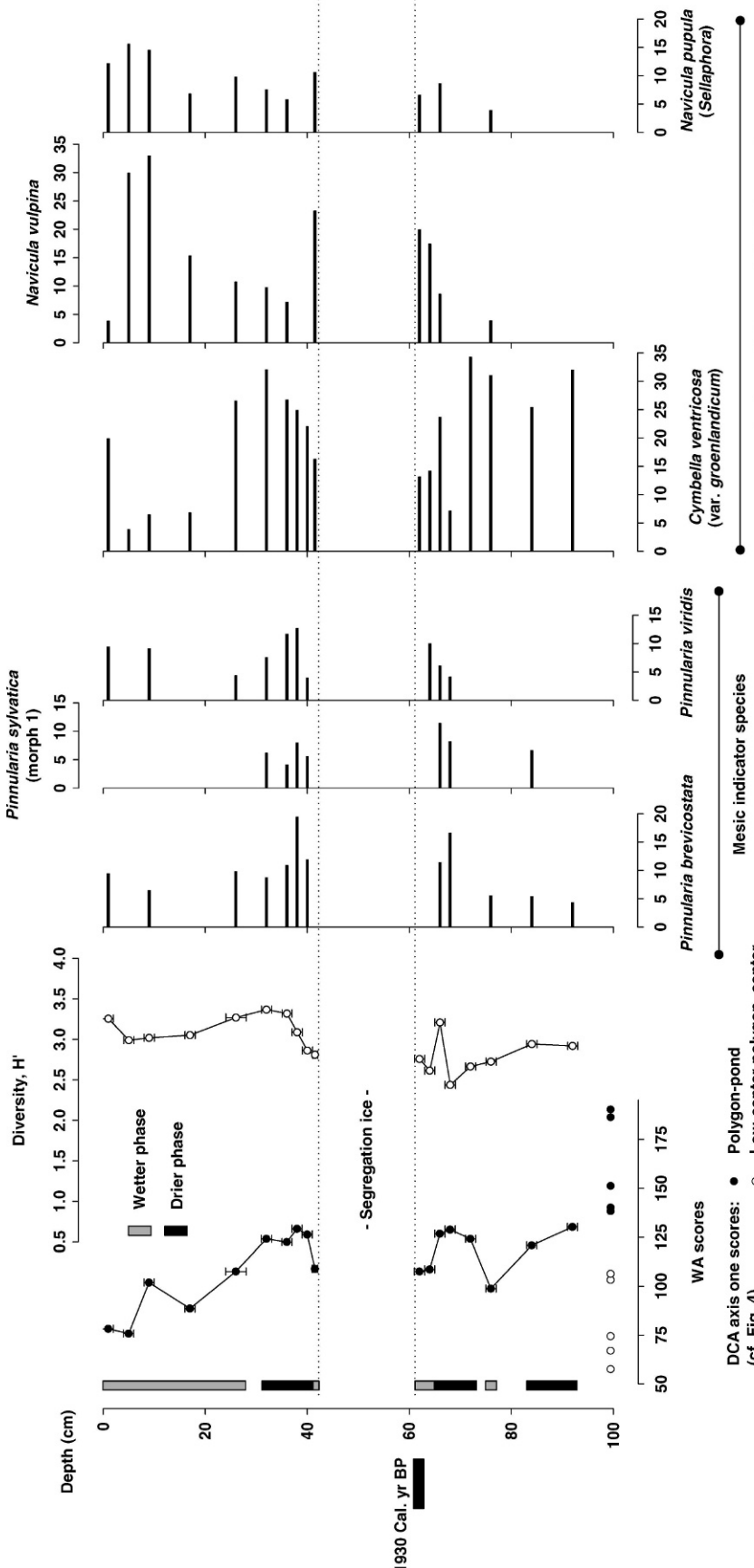

FIGURE 6. Stratigraphic record of WA scores (closed circles) and values of diversity H′ (open circles) for sub-fossil diatom assemblages in core BY-Pond. DCA axis one scores for diatom communities sampled from present-day polygon ponds and low-center polygon centers are aligned along the equivalent *x*-axis (WA scores) (cf. Fig. 5). Stratigraphic change in summary indicator taxa (% TDC) compares diatoms indicating mesic conditions (indicator species for low-center polygon flanks) with species indicating semi-aquatic and aquatic conditions: *Cymbella ventricosa* (var. *groenlandicum*) (low-center polygon centers), *Navicula vulpina* (polygon ponds), and *Navicula pupula* (*Sellaphora*) (thaw lakes) (cf. Fig. 4). Segregation ice and inferred wetter and drier phases are delimited; the position of a single radiocarbon date is plotted (cf. Table 1).

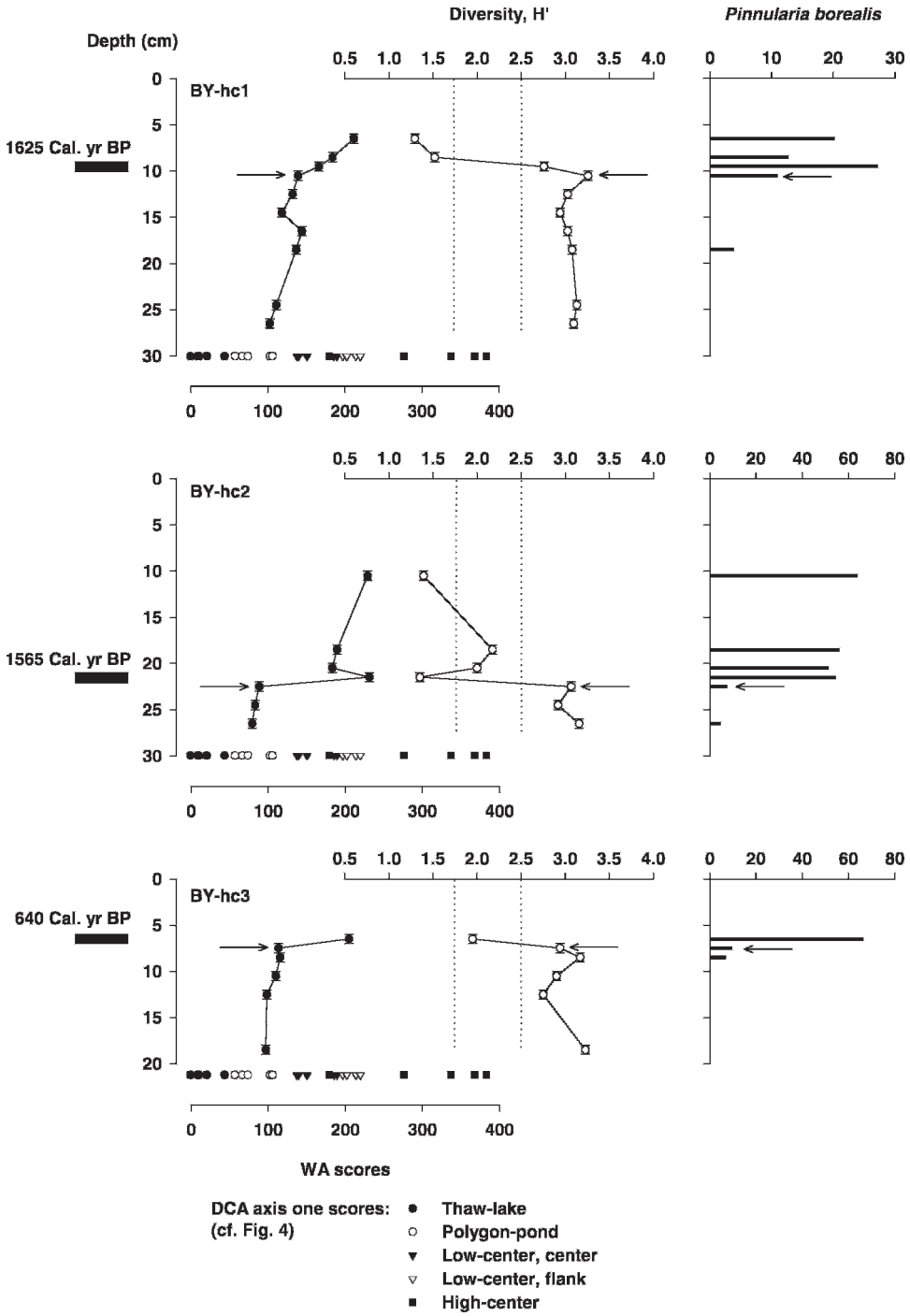

FIGURE 7. Stratigraphic record of WA scores (closed circles) and values of diversity H′ (open circles) for sub-fossil diatom assemblages in monoliths BY-hc1, -hc2, and -hc3, and change in % TDC for *Pinnularia borealis* (indicator species for high-center polygons; cf. Fig. 4). The lower threshold in values of H′ for analog low-center polygons, ponds, and thaw lakes, and the upper threshold in H′ for high-center polygons are delimited by two vertical dotted lines (cf. Fig. 5). DCA axis one scores for diatom communities sampled from present-day landform types are aligned along the equivalent *x*-axis (WA scores) (cf. Fig. 5). Transitions from wetter to drier conditions are indicated with an arrow; the positions of radiocarbon dates are plotted for each monolith (cf. Table 1).

tundra. Our results point instead to existing uncertainties which we believe highlight local effects underlying a dynamic and less predictable process of landform transition in patterned High Arctic wetlands. A more complete understanding of landform transitions in polygon wetlands is imperative in the context of global change. A great deal of research has focused on gradual climate-driven change in arctic vegetation, and consequences for ecosystem function (e.g. Arft et al., 1999; Bret-Harte et al., 2002; Epstein et al., 2000, 2004), and previous studies have identified the effect of relatively small changes in moisture content on the tundra carbon flux (Oechel et al., 1993, 1995; Weller et al., 1995). However, there is already evidence for major change in the spatial extent of contrasting tundra landforms (Stow et al., 2004) on a scale which heralds substantial implications for the tundra moisture regime and carbon cycling. These impacts include the potential for the large-scale degradation of permafrost (Beilman and Robinson, 2003; Lawrence and Slater, 2005), potentially resulting in widespread drainage and ice-wedge collapse (Jorgen-

son et al., 2006). A more robust framework describing landform transitions in polygon-patterned wetlands may now be needed to provide long-term context for existing and future landform change, and providing a background against which it may be possible to extrapolate climate impacts from short-term to long-term effects. We tentatively suggest that existing successional hypotheses may be inadequate to meet this challenge.

Acknowledgments

This research was funded by NSERC, FCAR, Centre d'études nordiques and Faculté des sciences des l'agriculture et de l'alimentation, Université Laval, as a university post-doctoral scholarship awarded to Christopher Ellis. Fieldwork was carried out from the Bylot Island Goose Camp, funded by a Canadian Wildlife Service Grant to Gilles Gauthier. We gratefully acknowledge logistic support and additional funding provided by Polar Continental Shelf Project. The Hunter and Trapper Association of Pond Inlet (Baffin Island) enabled access to Bylot Island.

References Cited

Aaby, B., and Digerfeldt, G., 1986: Sampling techniques for lakes and bogs. *In* Berglund, B. E. (ed.), *Handbook of Holocene Palaeoecology and Palaeohydrology*. Chichester: John Wiley & Sons, 181–194.

Allard, M., 1996: Geomorphological changes and permafrost dynamics: key factors in changing arctic ecosystems. An example from Bylot Island, Nunavut, Canada. *Geoscience Canada*, 23: 205–212.

Arft, A. M., Walker, M. D., Gurevitch, J., Alatalo, J. M., Bret-Harte, M. S., Dale, M., Diemer, M., Gugerli, F., Henry, G. H. R., Jones, M. H., Hollister, R. D., Jónsdóttir, I. S., Laine, K., Lévesque, E., Marion, G. M., Molau, U., Mølgaard, P., Nordenhäll, U., Raszhivin, V., Robinson, C. H., Starr, G., Stenström, A., Stenström, M., Totland, Ø., Turner, P. L., Walker, L. J., Webber, P. J., Welker, J. M., and Wookey, P. A., 1999: Responses of tundra plants to experimental warming: meta-analysis of the international tundra experiment. *Ecological Monographs*, 69: 491–511.

Battarbee, R. W., Jones, V. J., Flower, R. J., Cameron, N. G., Bennion, H., Carvalho, L., and Juggins, S., 2001: Diatoms. *In* Smol, J. P., Birks, H. J. B., and Last, W. M. (eds.), *Tracking Environmental Change Using Lake Sediments. DPER vol. 3*. Dordrecht: Kluwer Academic Publishers, 155–202.

Beilman, D. W., and Robinson, S. D., 2003: Peatland permafrost thaw and landform type along a climatic gradient. *In* Phillips, M., Springman, S. M., and Arenson, L. U. (eds.), *Proceedings of the 8th International Conference on Permafrost*. Zurich: Balkema, 61–65.

Billings, W. D., 1987: Carbon balance of Alaskan tundra and taiga ecosystems: past, present and future. *Quaternary Science Reviews*, 6: 165–177.

Billings, W. D., and Peterson, K. M., 1980: Vegetational change and ice-wedge polygons through the thaw-lake cycle in Arctic Alaska. *Arctic and Alpine Research*, 12: 413–432.

Billings, W. D., Luken, J. O., Mortensen, D. A., and Peterson, K. M., 1982: Arctic tundra: a source or sink for atmospheric carbon dioxide in a changing environment? *Oecologia*, 53: 7–11.

Billings, W. D., Luken, J. O., Mortensen, D. A., and Peterson, K. M., 1983: Increasing atmospheric carbon dioxide: possible effects on arctic tundra. *Oecologia*, 58: 286–289.

Bliss, L. C., 1997: Arctic ecosystems of North America. *In* Wielgolaski, F. E. (ed.), *Ecosystems of the World*. Amsterdam: Elsevier, 551–683.

Bliss, L. C., and Matveyeva, N., 1992: Circumpolar arctic vegetation. *In* Chapin, F. S., Jefferies, R. L., Reynolds, J. F., Shaver, G. R., and Svoboda, J. (eds.), *Arctic Ecosystems in a Changing Climate—An Ecophysiological Perspective*. San Diego: Academic Press, 59–89.

Bret-Harte, M. S., Shaver, G. R., and Chapin, F. S., 2002: Primary and secondary stem growth in arctic shrubs: implications for community response to environmental change. *Journal of Ecology*, 90: 251–267.

Britton, M. E., 1957: Vegetation of the Arctic tundra. *In* Hansen, H. P. (ed.), *Arctic Biology*. Corvallis: Oregon State University Press, 26–72.

Curtis, J. T., and McIntosh, R. P., 1950: The inter-relations of certain analytic and synthetic phytosociological characters. *Ecology*, 31: 434–455.

Curtis, J. T., and McIntosh, R. P., 1951: An upland forest continuum in the prairie-forest border region of Wisconsin. *Ecology*, 32: 476–496.

Dufrêne, M., and Legendre, P., 1997: Species assemblages and indicator species: the need for a flexible asymmetrical approach. *Ecological Monographs*, 67: 345–366.

Ellis, C. J., and Rochefort, L., 2004: Century-scale development of High Arctic polygon-patterned tundra wetland, Bylot Island (73°N). *Ecology*, 85: 963–978.

Ellis, C. J., and Rochefort, L., 2006: Long-term sensitivity of a High Arctic wetland to Holocene climate change. *Journal of Ecology*, 94: 441–454.

Epstein, H. E., Walker, M. D., Chapin, F. S., and Starfield, A. M., 2000: A transient nutrient-based model of arctic plant community response to climatic warming. *Ecological Applications*, 10: 824–841.

Epstein, H. E., Calef, M. P., Walker, M. D., Chapin, F. S., and Starfield, A. M., 2004: Detecting changes in arctic tundra plant communities in response to warming over decadal time scales. *Global Change Biology*, 10: 1325–1334.

Fallu, M.-A., Allaire, N., and Pienitz, R., 2000: *Freshwater Diatoms from Northern Québec and Labrador (Canada). Bibliotheca Diatomologica, Band 45*. Berlin/Stuttgart: Cramer, 200 pp.

Fortier, D., and Allard, M., 2004: Late Holocene syngenetic ice-wedge polygons development, Bylot Island, Canadian Arctic Archipelago. *Canadian Journal of Earth Sciences*, 41: 997–1012.

Fortier, D., Allard, A., and Pivot, F., 2006: A late-Holocene record of loess deposition in ice-wedge polygons reflecting wind activity and ground moisture conditions, Bylot Island, eastern Canadian Arctic. *The Holocene*, 16: 635–646.

Gajewski, K., Garneau, M., and Bourgeois, J. C., 1995: Palaeoenvironments of the Canadian High Arctic derived from pollen and plant macrofossils: problems and potentials. *Quaternary Science Reviews*, 14: 609–629.

Gorham, E., 1991: Northern peatlands: role in the carbon cycle and probable responses to climatic warming. *Ecological Applications*, 1: 182–195.

Harry, D. G., and Gozdzik, J. S., 1988: Ice wedges: growth, thaw transformation, and palaeoenvironmental significance. *Journal of Quaternary Science*, 3: 39–55.

Johnson, L. C., Shaver, G. R., Giblin, A. E., Nadelhoffer, K. J., Rastetter, E. R., Laundre, J. A., and Murray, G. L., 1996: Effects of drainage and temperature on carbon balance of tussock tundra microcosms. *Oecologia*, 108: 737–748.

Jorgenson, M. T., Shur, L., and Pullman, R., 2006: Abrupt increase in permafrost degradation in Arctic Alaska. *Geophysical Research Letters*, 33: L02503.

Klassen, R. A., 1993: *Quaternary geology and glacial history of Bylot Island, Northwest Territories*. Ottawa: Geological Survey of Canada, Memoir 429.

Krammer, K., and Lange-Bertalot, H., 1986: Bacillariophyceae. 1. Teil: Naviculaceae. *In* Ettl, H., Gerloff, J., Heynig, H., and Mollenhauer, D. (eds.), *Süßwasserflora von Mitteleuropa, Band 2/1*. Stuttgart/New York: Gustav Fischer Verlag.

Krammer, K., and Lange-Bertalot, H., 1988: Bacillariophyceae. 2. Teil: Bacillariaceae, Epithemiaceae, Surirellaceae. *In* Ettl, H., Gerloff, J., Heynig, H., and Mollenhauer, D. (eds.), *Süßwasser-*

flora von Mitteleuropa, Band 2/2. Stuttgart/New York: Gustav Fischer Verlag.

Krammer, K., and Lange-Bertalot, H., 1991a: Bacillariophyceae. 3. Teil: Centrales, Fragilariaceae, Eunotiaceae. *In* Ettl, H., Gerloff, J., Heynig, H., and Mollenhauer, D. (eds.), *Süßwasserflora von Mitteleuropa, Band 2/3*. Stuttgart/New York: Gustav Fischer Verlag.

Krammer, K., and Lange-Bertalot, H., 1991b: Bacillariophyceae. *4. Teil: Achnanthaceae, Kritische Ergänzungen zu Navicula (Lineolata) und Gomphonema. In* Ettl, H., Gerloff, J., Heynig, H., and Mollenhauer, D. (eds.), *Süßwasserflora von Mitteleuropa, Band 2/4*. Stuttgart/New York: Gustav Fischer Verlag.

Lachenbruch, A. H., 1966: Contraction theory of ice-wedge polygons: a qualitative discussion. *In*. National Academy of Sciences–National Research Council, *Proceedings of the First International Permafrost Conference*. Publication no. 1287:, 63–71.

Lawrence, D. M., and Slater, A. G., 2005: A projection of severe near-surface permafrost degradation during the 21st century. *Geophysical Research Letters*, 32: L24401.

Leffingwell, E., 1915: Ground-ice wedges. The dominant form of ground-ice on the north coast of Alaska. *Journal of Geology*, 23: 635–654.

Mackay, J. R., 1986: The first 7 years (1978–1985) of ice-wedge growth, Illisarvik experimental drained lake site, western Arctic coast. *Canadian Journal of Earth Sciences*, 23: 1782–1795.

Mackay, J. R., 1990: Some observations on the growth and deformation of epigenetic, syngenetic and anti-syngenetic ice wedges. *Permafrost and Periglacial Processes*, 1: 15–29.

Mackay, J. R., 1999: Periglacial features developed on the exposed lake bottoms of seven lakes that drained rapidly after 1950, Tuktoyaktuk Peninsula area, western Arctic coast, Canada. *Permafrost and Periglacial Processes*, 10: 39–63.

Mackay, J. R., 2000: Thermally induced movements in ice-wedge polygons, western Arctic coast: a long-term study. *Géographie physique et Quaternaire*, 54: 41–68.

Magurran, A. E., 2003: *Measuring Biological Diversity*. Oxford: Blackwell Publishing.

McCune, B., and Grace, J. B., 2002: *Analysis of Ecological Communities*. Gleneden Beach, Oregon: MjM Software Design.

McCune, B., and Mefford, M. J., 1999: *Pc-Ord, version 4*. Oregon: MjM Software Design.

Michaelson, G. J., Ping, C. L., and Kimble, J. M., 1996: Carbon storage and distribution in tundra soils of Arctic Alaska, U.S.A. *Arctic and Alpine Research*, 28: 414–424.

Oechel, W. C., and Vourtilis, G. L., 1994: The effects of climate change on land-atmosphere feedbacks in Arctic tundra regions. *Trends in Ecology and Evolution*, 9: 324–329.

Oechel, W. C., Hastings, S. J., Vourtilis, G., Jenkins, M., Riechers, G., and Grulke, N., 1993: Recent change of arctic tundra ecosystems from a net carbon dioxide sink to a source. *Nature*, 361: 520–523.

Oechel, W. C., Vourtilis, G. L., Hastings, S. J., and Bochkarev, S. A., 1995: Change in arctic CO_2 flux over two decades: effects of climate change at Barrow, Alaska. *Ecological Applications*, 5: 846–855.

Ovenden, L., 1982: Vegetation history of a polygonal peatland, northern Yukon. *Boreas*, 11: 209–224.

Péwé, T. L., 1966: Ice-wedges in Alaska—Classification, distribution and climatic significance. *In* National Academy of Sciences–National Research Council, *Proceedings of the First International Permafrost Conference*. Publication no. 1287:, 76–81.

Post, W. M., Emanuel, W. R., Zinke, P. J., and Stangenberger, A. G., 1982: Soil carbon pools and world life zones. *Nature*, 298: 156–159.

Seppälä, M., Gray, J. T., and Richard, P. J. H., 1991: Development of low-centred ice-wedge polygons in the northernmost Ungava Peninsula, Québec. *Boreas*, 20: 259–282.

Stow, D. A., Hope, A., McGuire, D., Verbyla, D., Gamon, J., Huemmrich, F., Houston, S., Racine, C., Sturm, M., Tape, K., Hinzman, L., Yoshikawa, K., Tweedie, C., Noyle, B., Silapaswan, C., Douglas, D., Griffith, B., Jia, G., Epstein, H., Walker, D., Daeschner, S., Petersen, A., Zhou, L., and Myneni, R., 2004: Remote sensing of vegetation and land-cover in arctic tundra ecosystems. *Remote Sensing of Environment*, 89: 281–308.

Stuiver, M., Burr, G. S., Hughen, K. A., Kromer, B., McCormac, G., Van der Plicht, J., Spurk, M., Reimer, P. J., Bard, E., and Beck, J. W., 1998: INTCAL98 radiocarbon age calibration, 24,000–0 cal BP. *Radiocarbon*, 40: 1041–1083.

Svoboda, J., and Henry, G. H. R., 1987: Succession in marginal arctic environments. *Arctic and Alpine Research*, 19: 373–384.

Tarnocai, C., and Zoltai, S. C., 1988: Wetlands of arctic Canada. *In* National Wetlands Working Group. (ed.), *Wetlands of Canada, Ecological Land Classification Series No. 24*. Montreal: Polyscience, 29–53.

Vardy, S. R., Warner, B. G., and Aravena, R., 1997: Holocene climate effects on the development of a peatland on the Tuktoyaktuk Peninsula, Northwest Territories. *Quaternary Research*, 47: 90–104.

Vardy, S. R., Warner, B. G., Turunen, J., and Aravena, R., 2000: Carbon accumulation in permafrost peatlands in the Northwest Territories and Nunavut, Canada. *The Holocene*, 10: 273–280.

Weller, G., Chapin, F. S., Everett, K. R., Hobbie, J. E., Kane, D., Oechel, W. C., Ping, C. L., Reeburgh, W. S., Walker, D., and Walsh, J., 1995: The arctic flux study: a regional view of trace gas release. *Journal of Biogeography*, 22: 365–374.

Zoltai, S. C., and Tarnocai, C., 1975: Perennially frozen peatlands in the Western Arctic and Subarctic of Canada. *Canadian Journal of Earth Sciences*, 12: 28–43.

MS accepted April 2008

APPENDIX 1

Diatom taxa recorded from habitats associated with present-day polygon landforms, their % frequency of occurrence (% TDC) in contrasting habitats (± 1 S.E.), and their DCA axis one score (cf. Fig. 4 and sample scores in Fig. 5).

	Mean % total diatom count ± 1 S.E.					
		Low-center polygons				
Taxon	High-center polygon	flanks	centers	Polygon-pond	Thaw-lakes	DCA axis one score
Amphora libyca	0 ± 0	0 ± 0	0 ± 0	1.57 ± 0.39	0.45 ± 0.24	−7.14
Caloneis silicula	0 ± 0	0 ± 0	0 ± 0	0.64 ± 0.23	1.5 ± 0.45	−25.61
Craticula cuspidata	0 ± 0	0 ± 0	0 ± 0	0.03 ± 0.03	1.5 ± 0.45	−2.04
Cymbella arctica	0 ± 0	0 ± 0	0 ± 0	2.02 ± 0.95	0.28 ± 0.09	−4.81
Cymbella hebridica	2.5 ± 2.5	0.71 ± 0.53	2.07 ± 1.06	4.55 ± 0.45	2.24 ± 0.93	95.91
Cymbella cf. *cistula*	0 ± 0	0 ± 0	0.05 ± 0.05	0.97 ± 0.29	0.51 ± 0.28	−5.61
Cymbella gracilis-lunata	0 ± 0	0.22 ± 0.16	1.52 ± 1.13	0 ± 0	0.03 ± 0.03	156.29
Cymbella incerta	0 ± 0	0 ± 0	0.45 ± 0.45	0.08 ± 0.05	0.16 ± 0.15	42.66
Cymbella cf. *lapponica*	0 ± 0	0.31 ± 0.16	4.89 ± 2.47	8 ± 2.58	0.26 ± 0.22	70.85
Cymbella cf. *obscura/ventricosa*	0 ± 0	0 ± 0	0.16 ± 0.16	9.56 ± 1.76	2.22 ± 0.66	3.66
Cymbella subcuspidata	0 ± 0	0 ± 0	0 ± 0	0.86 ± 0.01	1.12 ± 0.54	−7.73
Cymbella tynnii	0.31 ± 0.31	5.22 ± 1.64	3 ± 0.6	1.53 ± 0.79	0.5 ± 0.25	197.33
Cymbella ventricosa (var. *groenlandicum*)	0 ± 0	0.97 ± 0.43	7.79 ± 2.28	1.36 ± 0.92	0.19 ± 0.06	131.34
Diatoma spp. – *vulgaris* (morphotype *constricta*)	1.23 ± 1.23	0.94 ± 0.8	0.86 ± 0.43	1.36 ± 1.17	0.06 ± 0.06	291.65
Eunotia curtagrunowii	0 ± 0	0 ± 0	0.06 ± 0.06	0.04 ± 0.04	0.52 ± 0.19	−21.22
Eunotia cf. *diodon*	0 ± 0	0 ± 0	0 ± 0	0 ± 0	0.5 ± 0.19	−58.69
Eunotia cf. *lunaris/curvata*	0 ± 0	3.1 ± 0.55	2.1 ± 0.68	0.08 ± 0.08	0.03 ± 0.03	250.36
Eunotia praerupta (formerly *papilio*)	0 ± 0	0.62 ± 0.42	0.05 ± 0.03	0 ± 0	0 ± 0	292.26
Eunotia praerupta	11.4 ± 11.4	0.44 ± 0.27	0.98 ± 0.47	1.19 ± 0.52	1.63 ± 0.79	109.46
Eunotia pseudopectinalis	0 ± 0	0.31 ± 0.12	0.43 ± 0.4	0.29 ± 0.29	0.06 ± 0.06	176.19
Eunotia septentrionalis	0 ± 0	0.25 ± 0.19	0.6 ± 0.23	0 ± 0	0 ± 0	211.86
Eunotia spp.	0 ± 0	0.15 ± 0.09	0.88 ± 0.51	0.66 ± 0.43	4.56 ± 2.44	23.96
Fragilaria pinnata	0 ± 0	0 ± 0	0 ± 0	0 ± 0	21.28 ± 7.47	−73.83
Fragilaria sp. 1	0 ± 0	0 ± 0	0.05 ± 0.05	0 ± 0	5.43 ± 2.14	−69.01
Gomphonema acuminatum	0 ± 0	0 ± 0	0.05 ± 0.05	0.38 ± 0.29	0 ± 0	48.79
Gomphonema gracile	2.86 ± 2.86	0.15 ± 0.06	1.2 ± 0.63	0.53 ± 0.3	0.2 ± 0.09	134.82
Gomphonema lagerheimii	0 ± 0	0.06 ± 0.06	1.98 ± 0.98	2.07 ± 1.22	1.26 ± 0.61	26.2
Gomphonema parvulum	0 ± 0	0 ± 0	0.13 ± 0.08	0.03 ± 0.03	1.26 ± 0.32	−28.52
Hantzschia amphioxys	0 ± 0	1.19 ± 0.48	0.41 ± 0.16	0.21 ± 0.11	0.03 ± 0.03	200.87
Navicula cf. *elginensis* – type	0 ± 0	0 ± 0	0 ± 0	0 ± 0	2.21 ± 0.36	−71.7
Navicula jaernefeltii	0 ± 0	0 ± 0	0 ± 0	0.17 ± 0.12	2.64 ± 0.8	−54.52
Navicula pseudoscutiformis	0 ± 0	0 ± 0	0 ± 0	0 ± 0	3.76 ± 1.22	−73.37
Navicula pupula (Sellaphora)	0 ± 0	0 ± 0	0.1 ± 0.06	2.26 ± 0.84	2.96 ± 0.29	−16.13
Navicula radiosa	0 ± 0	0 ± 0	0.05 ± 0.05	2 ± 0.93	0.19 ± 0.13	19.6
Navicula vulpina	0 ± 0	0 ± 0	0 ± 0	4.18 ± 1.42	0.06 ± 0.04	11.33
Navicula sp. 1	0 ± 0	0 ± 0	0.17 ± 0.13	1.33 ± 0.39	0.03 ± 0.03	34.97
Neidium affine	0 ± 0	0 ± 0	0 ± 0	0.04 ± 0.04	0 ± 0	17.89
Neidium ampliatum	0 ± 0	0.68 ± 0.18	1.36 ± 0.66	0.32 ± 0.22	0.12 ± 0.06	144.82
Neidium bisulcatum	0 ± 0	1.76 ± 0.6	1.44 ± 0.61	0.81 ± 0.39	0.09 ± 0.06	173.14
Nitzschia spp.	2.81 ± 2.44	29.44 ± 4.31	39.42 ± 6.51	28.77 ± 5.06	6.87 ± 1.8	142.67
Pinnularia borealis	45.19 ± 15.46	0.31 ± 0.11	0 ± 0	0.07 ± 0.05	0.18 ± 0.08	429.88
Pinnularia brevicostata	0 ± 0	9.63 ± 3.02	3.24 ± 0.92	0.37 ± 0.22	0.26 ± 0.13	210.52
Pinnularia divergens	1.25 ± 1.25	0.47 ± 0.2	0.31 ± 0.14	0.23 ± 0.2	0.06 ± 0.04	292.5
Pinnularia gibba	0 ± 0	0.14 ± 0.14	0.54 ± 0.2	0.13 ± 0.05	0.09 ± 0.09	102.38
Pinnularia interrupta	0 ± 0	0 ± 0	0.25 ± 0.2	1.75 ± 0.46	1.18 ± 0.34	5.5
Pinnularia cf. *lagerstedtii*	0 ± 0	0 ± 0	0.03 ± 0.03	0 ± 0	0.49 ± 0.42	−38.77
Pinnularia microstauron	0.31 ± 0.31	3.3 ± 1.96	0.79 ± 0.33	2.68 ± 1.44	3.83 ± 1.41	104.58
Pinnularia cf. *rupestris*	0 ± 0	2.83 ± 0.55	0.18 ± 0.07	0.04 ± 0.04	1.48 ± 1.48	164.11
Pinnularia silvatica (morphotype 1)	2.81 ± 2.44	4.48 ± 1.76	1.43 ± 0.68	0.37 ± 0.21	0.12 ± 0.09	315.63
Pinnularia cf. *sinistra*	0 ± 0	0.55 ± 0.34	0 ± 0	0 ± 0	0.03 ± 0.03	273.77
Pinnularia cf. *subrostrata*	0 ± 0	3.49 ± 1.18	1.04 ± 0.4	0.37 ± 0.15	0.06 ± 0.06	225.06
Pinnularia viridis	0.62 ± 0.62	3.51 ± 1.07	0.63 ± 0.21	0.18 ± 0.14	0.15 ± 0.09	293.04
Pinnularia sp. 1	0 ± 0	3.26 ± 1.08	0.39 ± 0.32	0 ± 0	0.07 ± 0.05	268.38
Pinnularia sp. 2	0 ± 0	1.35 ± 0.61	1.65 ± 1.08	0.33 ± 0.24	0.36 ± 0.19	163.8
Pinnularia sp. 3	28.39 ± 10.3	8 ± 1.42	5.18 ± 1.69	2.39 ± 0.71	0.42 ± 0.15	317.7
Pinnularia sp. 4	0 ± 0	0 ± 0	0 ± 0	0 ± 0	0.44 ± 0.35	−88.73

(Continued)

APPENDIX 1

Continued.

Taxon	Mean % total diatom count ± 1 S.E.					DCA axis one score
		Low-center polygons				
	High-center polygon	flanks	centers	Polygon-pond	Thaw-lakes	
Stauroneis anceps	0 ± 0	0.13 ± 0.09	0.66 ± 0.25	1.42 ± 0.67	0.57 ± 0.2	48.58
Stauroneis phoenicenteron	0 ± 0	0.94 ± 0.24	2.95 ± 1.05	3.12 ± 0.69	0.48 ± 0.12	84.42
Stauroneis smithii	0 ± 0	0 ± 0	0 ± 0	0 ± 0	1.6 ± 0.96	−62.94
Tabellaria quadriseptata	0 ± 0	0 ± 0	0 ± 0	0.48 ± 0.34	0.06 ± 0.06	33.13
Tabellaria spp. – *flocculosa*	0 ± 0	0 ± 0	0.82 ± 0.76	0.49 ± 0.49	1.41 ± 0.33	1.8
chrysophyte cysts	2292.94 ± 655.8	44.61 ± 14.11	20.67 ± 1.33	7.38 ± 2.18	9.63 ± 1.77	–